



Published in final edited form as:

*Cell Stem Cell*. 2015 May 7; 16(5): 477–487. doi:10.1016/j.stem.2015.04.008.

## Myocardial infarction activates CCR2<sup>+</sup> hematopoietic stem and progenitor cells

Partha Dutta<sup>1,\*</sup>, Hendrik B. Sager<sup>1,\*</sup>, Kristy R. Stengel<sup>2</sup>, Kamila Naxerova<sup>3</sup>, Gabriel Courties<sup>1</sup>, Borja Saez<sup>4</sup>, Lev Silberstein<sup>4</sup>, Timo Heidt<sup>1</sup>, Matthew Sebas<sup>1</sup>, Yuan Sun<sup>1</sup>, Gregory Wojtkiewicz<sup>1</sup>, Paolo Fumene Feruglio<sup>1</sup>, Kevin King<sup>1</sup>, Joshua N. Baker<sup>5</sup>, Anja M. van der Laan<sup>6</sup>, Anna Borodovsky<sup>7</sup>, Kevin Fitzgerald<sup>6</sup>, Maarten Hulsmans<sup>1</sup>, Friedrich Hoyer<sup>1</sup>, Yoshiko Iwamoto<sup>1</sup>, Claudio Vinegoni<sup>1</sup>, Dennis Brown<sup>1</sup>, Marcelo Di Carli<sup>7</sup>, Peter Libby<sup>8</sup>, Scott Hiebert<sup>2</sup>, David Scadden<sup>3</sup>, Filip K. Swirski<sup>1</sup>, Ralph Weissleder<sup>1,10</sup>, and Matthias Nahrendorf<sup>1</sup>

<sup>1</sup>Center for Systems Biology, Massachusetts General Hospital and Harvard Medical School, Simches Research Building, 185 Cambridge St., Boston, MA 02114, USA <sup>2</sup>Department of Biochemistry, Vanderbilt School of Medicine, Nashville, TN 37235, USA <sup>3</sup>Edwin L. Steele Laboratory, Department of Radiation Oncology, Massachusetts General Hospital, 55 Fruit St, Boston, MA 02144 <sup>4</sup>Center for Regenerative Medicine, Massachusetts General Hospital, Simches Research Building, 185 Cambridge St., Boston, MA 02114, USA <sup>5</sup>Department of Cardiac Surgery, Massachusetts General Hospital, 55 Fruit St, Boston, MA 02144 <sup>6</sup>Department of Cardiology, Academic Medical Center, University of Amsterdam, PO Box 22660, Amsterdam, the Netherlands <sup>7</sup>Alnylam Pharmaceuticals, 300 Third Street, Cambridge, MA 02142 <sup>8</sup>Division of Nuclear Medicine and Molecular Imaging, Department of Radiology, Brigham and Women's Hospital, 75 Francis Street, Boston, MA 02115, USA <sup>9</sup>Cardiovascular Division, Department of Medicine, Brigham and Women's Hospital, 75 Francis Street, Boston, MA 02115, USA <sup>10</sup>Department of Systems Biology, Harvard Medical School, 200 Longwood Avenue, Boston, MA 02115, USA

### SUMMARY

© 2015 Published by Elsevier Inc.

Corresponding authors: Matthias Nahrendorf and Partha Dutta, Center for Systems Biology, 185 Cambridge Street, Boston, MA 02114, Tel: (617) 643-0500, Fax: (617) 643-6133, mnahrendorf@mgh.harvard.edu, dutta.partha@mgh.harvard.edu.

\*These authors contributed equally to this work

**Publisher's Disclaimer:** This is a PDF file of an unedited manuscript that has been accepted for publication. As a service to our customers we are providing this early version of the manuscript. The manuscript will undergo copyediting, typesetting, and review of the resulting proof before it is published in its final citable form. Please note that during the production process errors may be discovered which could affect the content, and all legal disclaimers that apply to the journal pertain.

#### SUPPLEMENTAL INFORMATION

The supplemental information contains five supplementary figures, two supplementary tables and a supplemental method section.

#### AUTHOR CONTRIBUTIONS

P.D. and H.B.S. designed and performed experiments, collected and analyzed the data and contributed to writing the manuscript, K.R.S., K.N., G.C., B.S., L.S., T.H., M.S., G.W., P.F.F., K.K., J.N.B., A.v.d.L., A.B., K.F., Y.S., M.H., F.H., Y.I., C.V., D.B., M.D., S.H., performed experiments, collected, analyzed and discussed data. K.N., D.S., P.L., F.K.S. and R.W. conceived experiments and discussed strategy and results. M.N. designed and managed the study and contributed to writing the manuscript, which was edited and approved by all co-authors.

#### CONFLICT OF INTEREST

A.B. and K.F. are Alnylam Pharmaceuticals employees. The remaining authors declare no competing financial interests.

Following myocardial infarction (MI), myeloid cells derived from the hematopoietic system drive a sharp increase in systemic leukocyte levels that correlate closely with mortality. The origin of these myeloid cells, and the response of hematopoietic stem and progenitor cells (HSPCs) to MI, however, is unclear. Here, we identify a CCR2<sup>+</sup>CD150<sup>+</sup>CD48<sup>-</sup> LSK hematopoietic subset as the most upstream contributor to emergency myelopoiesis after ischemic organ injury. CCR2<sup>+</sup> HSPC have fourfold higher proliferation rates than CCR2<sup>-</sup>CD150<sup>+</sup>CD48<sup>-</sup> LSK cells, display a myeloid differentiation bias, and dominate the migratory HSPC population. We further demonstrate the myeloid translocation gene 16 (Mtg16) regulates CCR2<sup>+</sup> HSPC emergence. Mtg16<sup>-/-</sup> mice have decreased levels of systemic monocytes and infarct-associated macrophages and display compromised tissue healing and post-MI heart failure. Together, these data provide insights into regulation of emergency hematopoiesis after ischemic injury, and identify potential therapeutic targets to modulate leukocyte output after MI.

---

## INTRODUCTION

Leukocytes, especially monocytes and macrophages, participate integrally in all stages of ischemic heart disease (Moore and Tabas, 2011) (Swirski and Nahrendorf, 2013). During atherogenesis, bone marrow-derived monocytes enter the vessel wall and give rise to macrophages and foam cells with tissue-destructive properties (Libby, 2002). Once a plaque ruptures, leukocytes massively accumulate in ischemic heart tissue, where they promote healing but may also worsen tissue damage if supplied in exaggerated numbers. An increase in circulating white cells promotes atherosclerosis, and myocardial infarction (MI) causes acute leukocytosis, which correlates closely with cardiovascular mortality (Swirski and Nahrendorf, 2013). How organ ischemia activates the hematopoietic system is poorly understood.

The majority of hematopoietic stem cells (HSC) are quiescent and enter the cell cycle only sparingly to self-renew and produce progeny (Wilson et al., 2008). Even though most HSC are dormant at any given time point, they can be activated by a systemic insult such as infection (Essers et al., 2009) (Baldrige et al., 2010) (Takizawa et al., 2011). Moreover, HSC are able to reversibly change between quiescence and proliferation states (Glauche et al., 2009). However, an “effector subset” that drives the proliferation response after a systemic insult has not been identified. We do not know how HSC respond to MI, which is the most common cause of death. The HSC response to tissue injury may be of particular relevance to patients that survive an ischemic insult because myeloid progeny plays a major role in tissue repair and patient recovery (Swirski and Nahrendorf, 2013). Here we describe a CD150<sup>+</sup> CD48<sup>-</sup> Lineage<sup>-</sup> Sca-1<sup>+</sup> c-Kit<sup>+</sup> (LSK) subset that can be identified by flow cytometry staining for the chemokine receptor CCR2 (CCR2<sup>+</sup> HSPC). After myocardial ischemic injury or exposure to bacterial lipopolysaccharide (LPS), CCR2<sup>-</sup> HSC remain quiescent while CCR2<sup>+</sup> HSPC replicate robustly. These observations identify the hematopoietic system's point of activation during severe stress and provide new insight into the pathogenesis of a highly prevalent disease.

## RESULTS

### MI triggers myelopoiesis in the bone marrow by activating CCR2<sup>+</sup> HSPC

Myocardial infarction results in leukocytosis and massive infiltration of myeloid cells into the injured heart (Swirski and Nahrendorf, 2013). Since myeloid cells in the infarct turn over in < 24 hours (Leuschner et al., 2012), the high demand must be met by hematopoietic organs, and new cells arise from hematopoietic stem and progenitor cells (HSPC). By following the bone marrow hematopoietic lineage upstream, we found increased proliferation of even the most primitive progenitor cells in mice with coronary ligation. In the femur, CD150<sup>+</sup> CD48<sup>-</sup> HSC (Figure 1A) and Lineage<sup>-</sup> Sca-1<sup>+</sup> c-Kit<sup>+</sup> cells (LSK) (Figure S1A) incorporate the highest levels of the proliferation marker BrdU 48 hours after MI. Because BrdU may be mitogenic (Takizawa et al., 2011), we confirmed this proliferation peak with cell cycle analysis on day 2 after coronary ligation while comparing to controls without ischemia. After MI, the percentage of quiescent HSC and LSK in G0 phase decrease while more HSC and LSK proliferate (G1 and S-G2-M phases) (Figure S1B,C). This results in more numerous HSC, LSK, multipotent progenitor cells (MPP) and lineage restricted progenitors (LRP) in the femur bone marrow on day 3 after MI (Figure S1D). <sup>18</sup>F-FLT-PET/CT, a clinical imaging method for measuring cellular proliferation in cancer (Shields et al., 1998), detected increased signal in mouse vertebrae, indicating that MI induces widespread bone marrow response (Figure 1B) and that imaging may be used to monitor hematopoiesis.

While the vast majority of HSC are quiescent, we hypothesized -- in line with recent reports on HSC heterogeneity in the steady state (Mossadegh-Keller et al., 2013; Oguro et al., 2013) -- that MI activates a specific HSC subset. Newly made monocytes rely on the chemokine receptor CCR2 for their departure from the bone marrow (Serbina and Pamer, 2006) and recruitment to the infarct (Dewald et al., 2005). CCR2 also identifies certain cardiac macrophage subsets (Epelman et al., 2014) and guides HSPC to the inflamed peritoneum (Si et al., 2010). We hypothesized that a CCR2<sup>+</sup> HSPC subset might give rise to the systemic increase in CCR2<sup>+</sup> leukocytes during myocardial infarction. Indeed, about 15% of CD48<sup>-</sup> CD150<sup>+</sup> HSC express CCR2 at high levels (Figure 1C). To test the specificity of FACS staining for CCR2, we examined HSC in CCR2<sup>+/RFP</sup> mice, in which we detected a similar RFP<sup>+</sup> HSC frequency of 15% (Figure S1E).

CCR2<sup>+</sup> CD150<sup>+</sup> CD48<sup>-</sup> LSK also contain higher levels of CCR2 mRNA when compared to their CCR2<sup>-</sup> counterparts (Figure S1E). CCR2<sup>+</sup> HSPC proliferate significantly more than CCR2<sup>-</sup> HSC in steady state, as assessed by BrdU incorporation (Figure 1D) and BrdU-independent cell cycle analysis (Figure S1F). 48 hours after coronary ligation, the gap in proliferative activity widens in these subsets; the fraction of BrdU<sup>+</sup> CCR2<sup>+</sup> HSPC increases to >40% whereas the fraction of BrdU<sup>+</sup> CCR2<sup>-</sup> HSC remains at low levels (Figure 1D). However, HSC proliferation in CCR2<sup>-/-</sup> mice was similar to that in wild type mice (Figure S1G). Analysis of human HSC harvested from the sternal bone marrow of patients (Table S1) undergoing median sternotomy for open heart surgery confirmed CCR2 expression by an HSC subset (Figure 2A) and the higher proliferation of CCR2<sup>+</sup> CD150<sup>+</sup> CD48<sup>-</sup> LSK (Figure 2B) observed in mice.

Electron microscopy revealed that murine  $CCR2^+ CD150^+ CD48^-$  LSK aggregate ribosomes (Figure 3A), indicating active protein synthesis (Hardesty et al., 1963) in association with increased cell proliferation. Depending on their proliferative activity, HSPC may reside in different bone marrow regions, with more primitive and quiescent cells locating to the vicinity of bone (Lo Celso et al., 2009; Nombela-Arrieta et al., 2013; Morrison and Scadden, 2014). Intravital microscopy after co-transfer of  $CCR2^-$  and  $CCR2^+ CD150^+ CD48^-$  LSK labeled with spectrally distinct fluorescent membrane dyes mapped the cells' distribution in the skull calvarium bone marrow. Matching their state of quiescence and activity, the majority of  $CCR2^-$  HSC reside near the endosteum, whereas  $CCR2^+$  HSPC are more distant (Figure 3B). We next examined similarities and differences between  $CCR2^+$  and  $CCR2^- CD150^+ CD48^-$  LSK sorted from steady state mouse bone marrow using Affymetrix microarrays. In a transcriptome-wide unsupervised hierarchical clustering analysis,  $CCR2^+$  and  $CCR2^- CD150^+ CD48^-$  LSK clearly segregated, pointing to global differences in their gene expression programs (Figure 3C and Table S2). As rescue capacity distinguishes HSC from hematopoietic progenitor cells, we investigated if  $CCR2^+ CD150^+ CD48^-$  LSK can rescue lethally irradiated mice. To this end, we injected lethally irradiated mice with either 100  $CCR2^-$  or 100  $CCR2^+ CD150^+ CD48^-$  LSK and Sca-1-depleted supportive bone marrow cells.  $CCR2^-$  HSC rescued 7/8 mice, whereas  $CCR2^+$  cells rescued 6/10 mice (Figure 3D). 120 days after first transplantation, both  $CCR2^-$  and  $CCR2^+ CD150^+ CD48^-$  LSK reconstitution gave rise to multilineage chimerism, which was biased towards the myeloid lineage in mice that received  $CCR2^+$  cells (Figure S2A). In a secondary host, which received either 100  $CCR2^-$  or  $CCR2^+ CD150^+ CD48^-$  LSK isolated from primary recipients,  $CCR2^+$  cells exhausted their self renewal capability while  $CCR2^-$  HSC did not (Figure S2B). In contrast to the primary host,  $CCR2^+ CD150^+ CD48^-$  LSK derived leukocyte chimerism was markedly reduced 5 weeks after secondary transplantation (Figure S2C). We used a limiting dilution assay to determine the number of functional HSC within  $CCR2^-$  or  $CCR2^+ CD48^- CD150^+$  LSK harvested from steady-state bone marrow (Figure 3E). Irradiated recipients received dilutions between 31 to 1,000 cells isolated by flow cytometry. Four months later, less than 0.1% multilineage blood chimerism determined the non-responding fraction of recipient mice. The frequency of functional HSC was 6.5-fold higher within  $CCR2^-$  HSC when compared to the  $CCR2^+$  subset (Figure 3E). However, a second limiting dilution assay indicated that the frequency of functional HSC is unchanged in  $CCR2^{-/-}$  bone marrow (Figure S2D). Altogether, these data suggest that  $CCR2^+$  HSPC represent a functionally distinct subset with reduced self renewal capacity in secondary hosts, and that this HSPC subset undergoes preferential activation during myocardial infarction. The data further implicate that  $CCR2$  may serve as a marker to identify this actively proliferating HSPC subset in mice and humans. However, genetic deficiency of  $CCR2$  alters neither HSC proliferation nor frequency.

### Myeloid translocation gene on chromosome 16 (Mtg16) activity in $CCR2^+$ HSPC

To understand the molecular mechanisms underlying the distinct functions of  $CCR2^+ CD150^+ CD48^-$  LSK, we contrasted their gene expression profiles with  $CCR2^- CD150^+ CD48^-$  LSK using gene set enrichment analysis. Of 78 gene sets that were upregulated in  $CCR2^+$  HSPC at a 25% false discovery rate (FDR) cutoff, the most significant set contained genes regulated by Mtg16, a transcriptional co-repressor required for hematopoietic

progenitor cell fate decisions and early progenitor cell proliferation (Chyla et al., 2008). Specifically, genes previously found downregulated in *Mtg16*<sup>-/-</sup> mouse bone marrow progenitor cells were enriched in CCR2<sup>+</sup> HSPC, while genes upregulated upon *Mtg16* knockout were enriched in CCR2<sup>-</sup> HSC (ranked as 4th significant among 1222 gene sets with a FDR<25%) (Figure 4A). We performed quantitative PCR to determine any difference in the subsets' expression of *Mtg16* or the transcription factors to which it binds (Hofmann et al., 2002; Okuda et al., 2001; Semerad et al., 2009; Summers et al., 2013; Young et al., 2004). CCR2<sup>+</sup> HSPC express significantly higher levels of *Mtg16* than CCR2<sup>-</sup> HSC (Figure 4B). Of the regulatory factors, *Prkar2a*, which increases in HSC of patients with myelodysplastic syndrome (Hofmann et al., 2002), was higher in CCR2<sup>+</sup> HSPC (Figure S3A). *Mtg16*<sup>-/-</sup> mice have fewer CCR2<sup>+</sup> HSPC while CCR2<sup>-</sup> HSC levels appear unchanged (Figure 4C). The paucity of CCR2<sup>+</sup> HSPC in *Mtg16*<sup>-/-</sup> mice associates with decreased HSC proliferation after MI (Figure S3B and C), and fewer monocytes and macrophages in the blood (Figure 4D) and infarct tissue (Figure 4E) on day 3 after coronary ligation. In line with this observation, *Mtg16* expression was higher in HSC during the active S-G2-M phases of the cell cycle in steady state (Figure S3D) and after a 5FU challenge (Figure S3E-G), indicating an association of *Mtg16* and cell proliferation. Of note, proliferating CCR2-deficient HSC are still able to increase *Mtg16* expression after myocardial infarction, demonstrating that CCR2 does not regulate *Mtg16* expression (Figure S3H). To evaluate their relative contribution to myelopoiesis after MI, we injected GFP<sup>+</sup> CCR2<sup>-</sup> or CCR2<sup>+</sup> CD150<sup>+</sup> CD48<sup>-</sup> LSK into CD45.1 mice on day 4 after coronary ligation. Four days after transfer, we investigated the progeny of transferred cells in the recipient's blood and infarcts (Figure 4F). We found significantly higher numbers of leukocytes produced by CCR2<sup>+</sup> CD150<sup>+</sup> CD48<sup>-</sup> LSK when compared to progeny of transferred CCR2<sup>-</sup> CD150<sup>+</sup> CD48<sup>-</sup> LSK. Almost all infarct leukocytes derived from CCR2<sup>+</sup> HSPC were myeloid cells (Figure 3F). These data indicate that CCR2<sup>+</sup> HSPC contribute to the infarct myeloid cell population; however, the functional implications for recovery after MI was still unclear. To explore this question, we investigated infarct healing in *Mtg16*<sup>-/-</sup> mice with severely reduced CCR2<sup>+</sup> CD150<sup>+</sup> CD48<sup>-</sup> LSK. Seven days after coronary ligation, protease activity, which is tightly linked to myeloid cell function, was lower in infarcts of *Mtg16*<sup>-/-</sup> mice (Figure 4G). Serial cardiac MRI reported a comparable infarct size on day 1 after coronary ligation in wild type and *Mtg16*<sup>-/-</sup> mice (Figure S3I), but left ventricular dilation accelerated in *Mtg16*<sup>-/-</sup> mice (Figure 4H). In parallel, immunoreactive staining for the macrophage surface marker CD68, myofibroblasts and collagen-1 decreased 7 days after coronary ligation in infarcts of *Mtg16*<sup>-/-</sup> mice (Figure S3J). Taken together, these data link an insufficient number of CCR2<sup>+</sup> HSPC with decreased macrophage supply to the ischemic wound, which impaired infarct healing and recovery after ischemic organ injury.

### Hierarchy and lineage bias

Gene set enrichment analysis indicated that CCR2<sup>-</sup> HSC express genes associated with upstream HSC (ranked 19th among 1222 significant gene sets) (Figure 5A), thereby suggesting these cells hold a higher hierarchical position. Principal components analysis of the whole transcriptome corroborates this observation: CCR2<sup>-</sup> HSC are in proximity to upstream CD34<sup>-</sup> LSK while CCR2<sup>+</sup> HSPC distribute closer to myeloid cells (Figure 5B). To test directly the subset's lineage relationships, we co-transferred CD45.2 CCR2<sup>-</sup> and CD45.1

CCR2<sup>+</sup> CD150<sup>+</sup> CD48<sup>-</sup> LSK into lethally irradiated mice and investigated reconstitution 4 months later. CCR2<sup>-</sup> HSC have a higher reconstitution capability and can generate CCR2<sup>+</sup> HSPC (Figure 5C). CCR2<sup>+</sup> HSPC failed to give rise to CCR2<sup>-</sup> HSC, confirming that CCR2<sup>-</sup> HSC are more primitive (Figure 5C). Since HSC harvested from CD45.2<sup>+</sup> mice engraft better than CD45.1 HSC (Purton and Scadden, 2007), we switched the HSC subtype's sources; however, CCR2<sup>-</sup> HSC still reconstituted better (data not shown). Slamf3 (CD229)<sup>-</sup> and Slamf4 (CD244)<sup>-</sup> HSC were previously classified as quiescent HSC (Oguro et al., 2013), and our observation that CCR2<sup>-</sup> HSC contain higher percentages of Slamf3<sup>-</sup> and Slamf4<sup>-</sup> cells (Figure S4A) supports that classification. In contrast to most multipotent progenitor cells (MPP) (Yang et al., 2005), CCR2<sup>+</sup> HSPC do not express FLK-2 (Figure S4B), which, together with expression of the SLAM family markers and long-term multilineage repopulation capacity in lethally irradiated mice, distinguishes CCR2<sup>+</sup> HSPC from downstream MPP on phenotypic and functional levels. After reconstituting irradiated recipients, CCR2<sup>+</sup> HSPC give rise to a higher percentage of CD11b<sup>+</sup> cells, which indicates their myeloid bias (Figure 5D and Figure S4C–E). Consistent with this finding, CCR2<sup>+</sup> HSPC express higher levels of the transcription factors PU.1 and Cebpa (Figure 5E). In contrast, CCR2<sup>-</sup> and CCR2<sup>+</sup> CD150<sup>+</sup> CD48<sup>-</sup> LSK comparably express Ikaros, a lymphoid transcription factor (Figure 5E).

### During MI bone marrow preferentially releases CCR2<sup>+</sup> HSC

CCR2 is involved in monocyte (Charo and Peters, 2003) and progenitor cell (Si et al., 2010) migration. Accordingly, genes associated with cellular migration are enriched in CCR2<sup>+</sup> CD150<sup>+</sup> CD48<sup>-</sup> LSK (ranked 9th out of 78 significant gene sets) (Figure 6A). Even though only 15% of bone marrow HSC express CCR2, most (>90%) LSK and HSC in the blood and spleen are CCR2<sup>+</sup> (Figure S5A). HSC release from the bone marrow follows circadian oscillations (Mendez- Ferrer et al., 2008) (Figure 6B), with a migration peak at noon (Zeitgeber 5). We found the majority of LSK released in steady state circadian oscillation express CCR2 at high levels (Figure 6B). To investigate HSC migration during steady state, we put CD45.2 and CD45.1 mice into parabiosis (Figure 6C and Figure S5B). After 5 weeks of joint circulation, we evaluated the expression of CCR2 on HSC that had migrated from one mouse to the bone marrow of the other. All CD45.1<sup>+</sup> parabiont-derived HSC in the bone marrow of CD45.2 mice expressed CCR2 at high levels (Figure 6C). Together, these data indicate that only CCR2<sup>+</sup> HSPC have migratory capacity in the steady state and confirm our adoptive transfer data (Figure 5C) showing that CCR2<sup>+</sup> HSPC do not revert to CCR2<sup>-</sup> HSC.

Post-MI HSPC release from the bone marrow enables extramedullary amplification of myelopoiesis and exacerbates inflammation in atherosclerotic plaque due to outsourced and accelerated splenic leukocyte production (Robbins et al., 2012) (Leuschner et al., 2012) (Dutta et al., 2012). Because we found that most migrating HSC are CCR2<sup>+</sup> during steady state, we tested whether infarct-induced HSC release also depends on CCR2. We induced MI in CCR2<sup>-/-</sup> mice and found impaired LSK release into blood (Figure 6D and Figure S5C). Knocking down CCR2 in HSC with lipidoid nanoparticle-delivered siRNA (Leuschner et al., 2011) reduces the MI-induced LSK release (Figure S5D–F) and consecutive splenic seeding (Figure S5G). In fact, siRNA may be an avenue for therapeutic intervention aiming to reduce the production and supply of inflammatory leukocytes. To

investigate further if  $CCR2^{-/-}$  LSK can leave the bone marrow, we generated mixed bone marrow chimeras by reconstituting lethally irradiated  $GFP^{+}$  mice with both  $CCR2^{-/-}$  and  $CCR2^{+/+}$  HSC (Figure 6E). Upon induction of MI, only  $CCR2^{+/+}$  LSK leave the bone marrow (Figure 6E). In wild type mice, the increase of circulating HSPC on day 3 after MI relies exclusively on  $CCR2^{+} CD150^{+} CD48^{-}$  LSK (Figure 6F). To investigate if stromal bone marrow cells produce more CCL2 after MI, we isolated endothelial and mesenchymal stem cells from the bone marrow on day 4 after coronary ligation, as both are potential sources for the chemokine (Shi et al., Immunity, 2011). After MI, only endothelial cells express elevated levels of CCL2 mRNA (Figure S5H), indicating that CCL2 produced by endothelial cells could mobilize  $CCR2^{+}$  HSPC from their niche.

### **CCR2<sup>+</sup> HSPC are activated after LPS and HMGB1 challenge**

Finally, we wondered if the role of  $CCR2^{+}$  HSPC is specific to myocardial infarction or whether this cell subset has broader functions. Thus, we challenged mice with LPS, an endotoxin contained in the cell walls of Gram-negative bacteria.  $CCR2^{+}$  HSPC expanded in the bone marrow 4 hours after injecting this Toll-like receptor ligand (Figure 7A). Measuring BrdU incorporation, we found that only  $CCR2^{+}$  HSPC increase proliferation after LPS challenge (Figure 7B). Preferential activation of  $CCR2^{+}$  HSPC at 4 hours after LPS injection suggests this subset expresses high levels of receptors that sense danger-associated molecular patterns (DAMPs). Accordingly,  $CCR2^{+}$  HSPC express significantly higher levels of TLR4 and TLR2 when compared to  $CCR2^{-}$  HSC (Figure 7C). In the context of cardiovascular disease, ischemic injury may release DAMPs that ligate TLRs. Indeed,  $CCR2^{+}$  HSPC increase TLR4 expression after MI (Figure S6A). Injection of HMGB1, which is released by cardiomyocytes during acute MI (Arslan et al., Nat Rev Cardiology, 2011), enhances  $CCR2^{+}$  HSPC proliferation (Figure S6B).

## **DISCUSSION**

The white blood count is one of the most frequently ordered medical tests, reflecting its clinical value. In cardiovascular patients, leukocytosis and monocytosis closely correlate with survival. We increasingly understand why: inflammatory monocytes and macrophages, when overproduced, damage the arterial wall and vital organs such as the heart after myocardial infarction or the brain after stroke. We have surprisingly limited understanding of mechanisms leading to increased leukocyte count in cardiovascular patients. Chronic leukocytosis affiliated with hyperlipidemia arises from perturbed cholesterol efflux, which makes hematopoietic progenitors cycle more vigorously (Yvan-Charvet et al., 2010) and gives rise to progressively elevated monocyte counts in mice with atherosclerosis (Swirski et al., 2006) (Tacke et al., 2007). Myocardial infarction induces enhanced extramedullary myelopoiesis due to increased progenitor cell traffic between the marrow and the spleen (Dutta et al., 2012). Even though insufficient and exuberant leukocyte production after myocardial infarction associates with poorer prognosis (Nahrendorf et al., Circulation 2010), the mechanisms that link ischemic injury to changes in hematopoiesis at the stem cell level have remained obscure.

This study identifies preferential activation of a CCR2<sup>+</sup> CD150<sup>+</sup> CD48<sup>-</sup> LSK subset during myocardial infarction or exposure to a bacterial danger signal, LPS. In contrast, CCR2<sup>-</sup> CD150<sup>+</sup> CD48<sup>-</sup> LSK remain quiescent in stress conditions. Thus, CCR2<sup>+</sup> CD48<sup>-</sup> CD150<sup>+</sup> LSK represent the most upstream point of increased myelopoiesis after MI. In distinction to retrospectively identifiable myeloid-restricted progenitors with long-term repopulation activity (Yamamoto et al., 2013), CCR2 serves as a cell surface marker to prospectively identify a highly active cell population within the CD150<sup>+</sup> CD48<sup>-</sup> SLAM gate. CCR2 also participates functionally by mediating migratory cell activity during myocardial infarction. A few HSPC migrate even in the steady state, possibly to survey peripheral organs (Massberg et al., 2007). Of direct relevance to the present observations, CCR2<sup>+</sup> cells dominate in this migratory population. Moreover, CCR2<sup>+</sup> HSPC express receptors of danger associated molecular patterns (DAMPs) such as TLR4 and TLR2. They increase expression of these receptors further after MI, rendering them sensitive to danger signals, such as HMGB1, released from the dead myocardium. In addition, CCR2<sup>+</sup> CD150<sup>+</sup> CD48<sup>-</sup> LSK are also preferentially activated after LPS challenge.

After myocardial infarction, activity of the sympathetic nervous system triggers bone marrow release of HSPC into circulation in larger numbers, thus enabling the outsourcing of inflammatory cell production to the spleen (Dutta et al., 2012). Splenic myelopoiesis replenishes the organ's monocyte reservoir which supplies cells in the first 24 hours after injury (Swirski et al., 2009) but also supports continued contribution of cells to the heart (Leuschner et al., 2012). In healing infarcts and other wounds, the initial need for macrophages is followed by the necessity for resolution of inflammation. The observation of impaired infarct healing in *Mtg16*<sup>-/-</sup> mice with an insufficient supply of infarct macrophages underscores the cell's contribution to tissue repair. However, if inflammation resolution is delayed, infarcts rupture and heart failure occurs. Thus, the supply of inflammatory cells, which are initially important for clearing of dead cells and orchestration of tissue repair, should wind down as wound healing progresses to proliferative stages. The post-MI bone marrow release of CCR2<sup>+</sup> CD150<sup>+</sup> CD48<sup>-</sup> LSK, which excel at migration and myeloid cell production but have a lower self renewal capacity than CCR2<sup>-</sup> CD150<sup>+</sup> CD48<sup>-</sup> LSK, may hypothetically amount to a program of expanded leukocyte production with a built-in exit strategy. If likewise released, CCR2<sup>-</sup> HSC would ignite indefinite extramedullary hematopoiesis and thus perpetuate systemic inflammation, a complication that is likely avoided by limiting bone marrow cell exit to CCR2<sup>+</sup> HSPC which we found to exhaust in secondary transplantation assays.

Since CCR2<sup>+</sup> CD150<sup>+</sup> CD48<sup>-</sup> LSK do not rescue secondary hosts, they are not long-term HSC. CCR2<sup>+</sup> CD150<sup>+</sup> CD48<sup>-</sup> LSK share phenotypic markers with short-term HSC, as they express CD34 but not FLK2, and resemble short-term HSC in their failure to repopulate secondary hosts (Yang et al., 2005). CCR2<sup>+</sup> CD150<sup>+</sup> CD48<sup>-</sup> LSK generate multilineage chimerism in primary recipients 4 months after reconstitution and rescue lethally irradiated primary hosts, which places them functionally above short-term HSC according to some definitions (Reya et al., 2001) (Challen et al., 2009); however, they resemble recently described upstream MPP-1 (Cabezas-Wallscheid et al., 2014). We therefore refer to these cells as “CCR2<sup>+</sup> HSPC”.



Unchanged functional HSC frequency and proliferation in *CCR2*<sup>-/-</sup> mice indicates that CCR2 does not regulate stem cell replication after MI. Rather, we identify Mtg16 as a molecular decision node in HSPC and, consecutively, in monocyte production. The dampened post-MI myelopoiesis and compromised infarct healing in *Mtg16*<sup>-/-</sup> mice may be caused by the lack of the CCR2<sup>+</sup> HSPC subset but could additionally reflect compromised responses of downstream progenitors. Despite growing evidence of inflammation's importance in ischemic heart disease, specific anti-inflammatory therapeutic approaches have only begun to emerge. The data presented here indicate that targeting CCR2<sup>+</sup> HSPC, for instance via CCR2 or Mtg16, might reduce emergency monocyte production, curb macrophage oversupply and limit excessive tissue destruction during acute inflammation triggered by ischemic injury.

## EXPERIMENTAL PROCEDURES

### Animal models and surgeries

All mouse studies were approved by the Subcommittee on Animal Research Care at Massachusetts General Hospital. C57BL/6J, C57BL/6-Tg(UBC-GFP)30Scha/J, B6. SJL-Ptprca<sup>a</sup> Pepcb<sup>b</sup>/BoyJ (CD45.1), B6.129S4-*Ccr2*<sup>tm1fc/J</sup> (*CCR2*<sup>-/-</sup>) and B6.129(Cg)-*Ccr2*<sup>tm2.11fc/J</sup> (*CCR2*<sup>+RFP</sup>) mice were purchased from Jackson Laboratory. For all experiments, 4–5 months old mice were used. To induce myocardial infarction, thoracotomy in the fourth left intercostal space was performed after intubation and ventilation with 2% isoflurane. The left coronary artery was permanently ligated with a monofilament nylon 8-0 suture, and the thorax was closed with a 5-0 suture. For parabiosis, an incision was made on the skin on the lateral sides of mice starting from the ear reaching the tail. Corresponding scapulae were joined using a 6-0 suture. A 0.5 cm incision was made on the abdomen and approximated with 6-0 suture. The skin was sutured with mono-nylon 6-0 (Ethicon).

### Flow cytometry

Cells diluted in 300 µl of FACS buffer were stained with fluorochrome labelled antibodies against mouse leukocyte markers and hematopoietic stem and progenitor cell markers. For leukocyte staining, a phycoerythrin (PE) lineage cocktail was used, which contains antibodies directed against CD90 (clone 53-2.1), B220 (clone RA3-6B2), CD49b (clone DX5), NK1.1 (clone PK136), Ly-6G (clone 1A8) and Ter-119 (clone TER-119). Leukocytes were stained with antimouse CD11b (clone M1/70), CD11c (clone HL3), F4/80 (clone BM8) and Ly6C (clone AL-21). Monocytes were identified as (CD90/B220/ CD49b/NK1.1/Ly-6G/Ter119)<sup>low</sup> CD11b<sup>high</sup> F4/80<sup>low</sup> CD11c<sup>neg/low</sup> Ly-6C<sup>high/low</sup>. For stem and progenitor cell staining, we used biotin-conjugated antibodies against CD11b (clone M1/70), CD11c (clone N418), and IL7Rα (clone A7R34) in addition to the lineage antibodies used for leukocyte staining. The cells were then stained with anti c-Kit (clone 2B8), Sca-1 (clone D7), CD16/32 (clone 2.4G2), CD34 (clone RAM34), CD115 (clone AFS98), CD150 (9D1), CD48 (HM48-1) and CCR2 (RandD Biosystems clone: 475301; abcam: ab21667). Hematopoietic Stem Cells (HSC) were identified as lineage<sup>low</sup> c-Kit<sup>high</sup> Sca-1<sup>high</sup> CD150<sup>+</sup>CD48<sup>-</sup>. Downstream progenitors such as lineage restricted progenitor (LRP) and multi potent progenitor (MPP) were identified as lineage<sup>low</sup> c-Kit<sup>high</sup> Sca-1<sup>high</sup> CD150<sup>-</sup>CD48<sup>+</sup> and lineage<sup>low</sup> c-Kit<sup>high</sup> Sca-1<sup>high</sup> CD150<sup>-</sup>CD48<sup>-</sup>, respectively.

## Microarray experiments and data analysis

For each sample, HSC sorted from 20 B6 mice were pooled, and RNA was extracted as described above. cDNA was prepared using the Ovation Pico WTA System V2 (NuGEN) and hybridized to GeneChip® Mouse Gene 2.0 ST arrays (Affymetrix). Raw data were normalized using the robust multi-array average (Irizarry et al., 2003) and are available at Gene Expression Omnibus under accession number GSE53827. We eliminated probe sets with low variance across all samples (lower quartile) and performed hierarchical clustering using Euclidian distance and Ward's method. Differentially expressed genes were determined using Significance Analysis of Microarrays (Tusher et al., 2001). Probe sets with a false discovery rate below 10% are provided in Supplementary Table 1. We performed gene set enrichment analysis (Subramanian et al., 2005) with default parameters, except that we used class difference as a ranking metric and permuted gene sets instead of phenotype labels. To determine how the transcriptome of CCR2<sup>+</sup> and CCR2<sup>-</sup> CD150<sup>+</sup> CD48<sup>-</sup> LSK relates to gene expression in various other hematopoietic cells, we used a previously published method (Kho et al., 2004) based on principal components analysis to integrate our data with a reference data set containing expression profiles of hematopoietic cells at different stages of differentiation (ranging from CD34<sup>-</sup> HSCs to fully differentiated myeloid and lymphoid cells). Briefly, we obtained reference data from Konuma et al. (Konuma et al., 2011) (GEO Accession number GSE27787) and collapsed both data sets to gene symbols, retaining only genes that were present in both arrays. We then performed a principal components analysis of the reference data set and used the first two principal components to project both the Konuma data and our CCR2<sup>+/-</sup> gene expression profiles into a two-dimensional space.

## siRNA treatment

siRNA (5-uGcuAAAcGucucuGcAAAdTsdT-3 (sense), 5-UUUGcAGAGACGUUuAGcAdTsdT-3 (anti-sense)) against CCR2 was formulated into lipid nanoparticles as described previously (Leuschner et al., 2011). B6 mice were injected intravenously with 0.5mg/kg/day siRNA for 4 days after MI.

## Supplementary Material

Refer to Web version on PubMed Central for supplementary material.

## ACKNOWLEDGEMENTS

We thank Michael Waring and Adam Chicoine from Ragon Institute (of MGH, MIT and Harvard), and Laura Prickett-Rice, Kat Folz-Donahue and Meredith Weglarz from the Flow Cytometry Core Facility (Massachusetts General Hospital, Center for Regenerative Medicine and Harvard Stem Cell Institute) for assistance with cell sorting. We also acknowledge Dr. Chee Lim, Vanderbilt Medical Center MMPC (supported by U24 DK059637) for help with infarct surgery. We thank Mary McKee (Program in Membrane Biology Microscopy) for help with electron microscopy. This work was funded in part by grants from the National Institute of Health R01-HL096576, R01-HL117829, R01-NS084863 (M.N.); HHSN268201000044C (R.W.), K99-HL121076 (P.D.). Hendrik B. Sager and Timo Heidt are funded by Deutsche Forschungsgemeinschaft (SA1668/2-1 to H.B.S and HE-6382/1-1 to T.H.). Support for the Program in Membrane Biology Microscopy Core comes from the Boston Area Diabetes and Endocrinology Research Center (DK57521) and the MGH Center for the Study of Inflammatory Bowel Disease (DK43351).

## REFERENCES

- Arslan F, de Kleijn DP, Pasterkamp G. Innate immune signaling in cardiac ischemia. *Nature Reviews Cardiology*. 2011; 8:292–300.
- Baldrige MT, King KY, Boles NC, Weksberg DC, Goodell MA. Quiescent haematopoietic stem cells are activated by IFN-gamma in response to chronic infection. *Nature*. 2010; 465:793–797. [PubMed: 20535209]
- Cabezas-Wallscheid N, Klimmeck D, Hansson J, Lipka DB, Reyes A, Wang Q, Weichenhan D, Lier A, von Paleske L, Renders S, Wünsche P, Zeisberger P, Brocks D, Gu L, Herrmann C, Haas S, Essers MA, Brors B, Eils R, Huber W, Milsom MD, Plass C, Krijgsveld J, Trumpp A. Identification of regulatory networks in HSCs and their immediate progeny via integrated proteome, transcriptome, and DNA Methylation analysis. *Cell Stem Cell*. 2014 Oct 2; 15(4):507–22. 2014. [PubMed: 25158935]
- Challen GA, Boles N, Lin KK, Goodell MA. Mouse hematopoietic stem cell identification and analysis. *Cytometry A*. 2009; 75:14–24. [PubMed: 19023891]
- Charo IF, Peters W. Chemokine receptor 2 (CCR2) in atherosclerosis, infectious diseases, and regulation of T-cell polarization. *Microcirculation*. 2003; 10:259–264. [PubMed: 12851643]
- Chyla BJ, Moreno-Miralles I, Steapleton MA, Thompson MA, Bhaskara S, Engel M, Hiebert SW. Deletion of Mtg16, a target of t(16;21), alters hematopoietic progenitor cell proliferation and lineage allocation. *Mol Cell Biol*. 2008; 28:6234–6247. [PubMed: 18710942]
- Courties G, Heidt T, Sebas M, Iwamoto Y, Jeon D, Truelove J, Tricot B, Wojtkiewicz G, Dutta P, Sager HB, Borodovsky A, Novobrantseva T, Klebanov B, Fitzgerald K, Anderson DG, Libby P, Swirski FK, Weissleder R, Nahrendorf M. In vivo silencing of the transcription factor IRF5 reprograms the macrophage phenotype and improves infarct healing. *J Am Coll Cardiol*. 2014; 63:1556–1566. [PubMed: 24361318]
- Dewald O, Zymek P, Winkelmann K, Koerting A, Ren G, Abou-Khamis T, Michael LH, Rollins BJ, Entman ML, Frangogiannis NG. CCL2/Monocyte Chemoattractant Protein-1 regulates inflammatory responses critical to healing myocardial infarcts. *Circ Res*. 2005; 96:881–889. [PubMed: 15774854]
- Dutta P, Courties G, Wei Y, Leuschner F, Gorbatov R, Robbins CS, Iwamoto Y, Thompson B, Carlson AL, Heidt T, Majmudar MD, Lasitschka F, Etzrodt M, Waterman P, Waring MT, Chicoine AT, van der Laan AM, Niessen HW, Piek JJ, Rubin BB, Butany J, Stone JR, Katus HA, Murphy SA, Morrow DA, Sabatine MS, Vinegoni C, Moskowitz MA, Pittet MJ, Libby P, Lin CP, Swirski FK, Weissleder R, Nahrendorf M. Myocardial infarction accelerates atherosclerosis. *Nature*. 2012; 487:325–329. [PubMed: 22763456]
- Epelman S, Lavine KJ, Beaudin AE, Sojka DK, Carrero JA, Calderon B, Brija T, Gautier EL, Ivanov S, Satpathy AT, Schilling JD, Schwendener R, Sergin I, Razani B, Forsberg EC, Yokoyama WM, Unanue ER, Colonna M, Randolph GJ, Mann DL. Embryonic and adult-derived resident cardiac macrophages are maintained through distinct mechanisms at steady state and during inflammation. *Immunity*. 2014; 40:91–104. [PubMed: 24439267]
- Essers MA, Offner S, Blanco-Bose WE, Waibler Z, Kalinke U, Duchosal MA, Trumpp A. IFN $\alpha$  activates dormant haematopoietic stem cells in vivo. *Nature*. 2009; 458:904–908. [PubMed: 19212321]
- Glauche I, Moore K, Thielecke L, Horn K, Loeffler M, Roeder I. Stem cell proliferation and quiescence--two sides of the same coin. *PLoS Comput Biol*. 2009; 5:e1000447. [PubMed: 19629161]
- Hardesty B, Hutton JJ, Arlinghaus R, Schweet R. Polyribosome formation and hemoglobin synthesis. *Proc Natl Acad Sci U S A*. 1963; 50:1078–1085. [PubMed: 14096181]
- Hofmann WK, de Vos S, Komor M, Hoelzer D, Wachsman W, Koeffler HP. Characterization of gene expression of CD34+ cells from normal and myelodysplastic bone marrow. *Blood*. 2002; 100:3553–3560. [PubMed: 12411319]
- Irizarry RA, Hobbs B, Collin F, Beazer-Barclay YD, Antonellis KJ, Scherf U, Speed TP. Exploration, normalization, and summaries of high density oligonucleotide array probe level data. *Biostatistics*. 2003; 4:249–264. [PubMed: 12925520]

- Kho AT, Zhao Q, Cai Z, Butte AJ, Kim JY, Pomeroy SL, Rowitch DH, Kohane IS. Conserved mechanisms across development and tumorigenesis revealed by a mouse development perspective of human cancers. *Genes Dev.* 2004; 18:629–640. [PubMed: 15075291]
- Konuma T, Nakamura S, Miyagi S, Negishi M, Chiba T, Oguro H, Yuan J, Mochizuki-Kashio M, Ichikawa H, Miyoshi H, Vidal M, Iwama A. Forced expression of the histone demethylase Fbx110 maintains self-renewing hematopoietic stem cells. *Exp Hematol.* 2011; 39:697–709. e5. [PubMed: 21540074]
- Leuschner F, Dutta P, Gorbato R, Novobrantseva TI, Donahoe JS, Courties G, Lee KM, Kim JI, Markmann JF, Marinelli B, Panizzi P, Lee WW, Iwamoto Y, Milstein S, Epstein-Barash H, Cantley W, Wong J, Cortez-Retamozo V, Newton A, Love K, Libby P, Pittet MJ, Swirski FK, Kotliansky V, Langer R, Weissleder R, Anderson DG, Nahrendorf M. Therapeutic siRNA silencing in inflammatory monocytes in mice. *Nat Biotechnol.* 2011; 29:1005–1010. [PubMed: 21983520]
- Leuschner F, Rauch PJ, Ueno T, Gorbato R, Marinelli B, Lee WW, Dutta P, Wei Y, Robbins C, Iwamoto Y, Sena B, Chudnovskiy A, Panizzi P, Keliher E, Higgins JM, Libby P, Moskowitz MA, Pittet MJ, Swirski FK, Weissleder R, Nahrendorf M. Rapid monocyte kinetics in acute myocardial infarction are sustained by extramedullary monocytopoiesis. *J Exp Med.* 2012; 209:123–137. [PubMed: 22213805]
- Libby P. Inflammation in atherosclerosis. *Nature.* 2002; 420:868–874. [PubMed: 12490960]
- Lo Celso C, Fleming HE, Wu JW, Zhao CX, Miake-Lye S, Fujisaki J, Cote D, Rowe DW, Lin CP, Scadden DT. Live-animal tracking of individual haematopoietic stem/progenitor cells in their niche. *Nature.* 2009; 457:92–96. [PubMed: 19052546]
- Massberg S, Schaerli P, Knezevic-Maramica I, Kollnberger M, Tubo N, Moseman EA, Huff IV, Jung T, Wagers AJ, Mazo IB, von Andrian UH. Immunosurveillance by hematopoietic progenitor cells trafficking through blood, lymph, and peripheral tissues. *Cell.* 2007; 131:994–1008. [PubMed: 18045540]
- Mendez-Ferrer S, Lucas D, Battista M, Frenette PS. Haematopoietic stem cell release is regulated by circadian oscillations. *Nature.* 2008; 452:442–447. [PubMed: 18256599]
- Moore KJ, Tabas I. Macrophages in the pathogenesis of atherosclerosis. *Cell.* 2011; 145:341–355. [PubMed: 21529710]
- Morrison SJ, Scadden DT. The bone marrow niche for haematopoietic stem cells. *Nature.* 2014; 505:327–334. [PubMed: 24429631]
- Mossadegh-Keller N, Sarrazin S, Kandalla PK, Espinosa L, Stanley ER, Nutt SL, Moore J, Sieweke MH. M-CSF instructs myeloid lineage fate in single haematopoietic stem cells. *Nature.* 2013; 497:239–243. [PubMed: 23575636]
- Nahrendorf M, Pittet MJ, Swirski FK. Monocytes: protagonists of infarct inflammation and repair after myocardial infarction. *Circulation.* 2010; 121:2437–2445. [PubMed: 20530020]
- Nahrendorf M, Waterman P, Thurber G, Groves K, Rajopadhye M, Panizzi P, Marinelli B, Aikawa E, Pittet MJ, Swirski FK, Weissleder R. Hybrid in vivo FMT-CT imaging of protease activity in atherosclerosis with customized nanosensors. *Arterioscler Thromb Vasc Biol.* 2009; 29:1444–1451. [PubMed: 19608968]
- Nombela-Arrieta C, Pivarnik G, Winkel B, Canty KJ, Harley B, Mahoney JE, Park SY, Lu J, Protopopov A, Silberstein LE. Quantitative imaging of haematopoietic stem and progenitor cell localization and hypoxic status in the bone marrow microenvironment. *Nat Cell Biol.* 2013; 15:533–543. [PubMed: 23624405]
- Oguro H, Ding L, Morrison SJ. SLAM family markers resolve functionally distinct subpopulations of hematopoietic stem cells and multipotent progenitors. *Cell Stem Cell.* 2013; 13:102–116. [PubMed: 23827712]
- Okuda T, Nishimura M, Nakao M, Fujita Y. RUNX1/AML1: a central player in hematopoiesis. *Int J Hematol.* 2001; 74:252–257. [PubMed: 11721959]
- Pang WW, Price EA, Sahoo D, Beerman I, Maloney WJ, Rossi DJ, Schrier SL, Weissman IL. Human bone marrow hematopoietic stem cells are increased in frequency and myeloid-biased with age. *Proc Natl Acad Sci U S A.* 2011; 108:20012–20017. [PubMed: 22123971]

- Purton LE, Scadden DT. Limiting factors in murine hematopoietic stem cell assays. *Cell Stem Cell*. 2007; 1:263–270. [PubMed: 18371361]
- Reya T, Morrison SJ, Clarke MF, Weissman IL. Stem cells, cancer, and cancer stem cells. *Nature*. 2001; 414:105–111. [PubMed: 11689955]
- Robbins CS, Chudnovskiy A, Rauch PJ, Figueiredo JL, Iwamoto Y, Gorbato R, Etzrodt M, Weber GF, Ueno T, van Rooijen N, Mulligan-Kehoe MJ, Libby P, Nahrendorf M, Pittet MJ, Weissleder R, Swirski FK. Extramedullary hematopoiesis generates Ly-6C(high) monocytes that infiltrate atherosclerotic lesions. *Circulation*. 2012; 125:364–374. [PubMed: 22144566]
- Semerad CL, Mercer EM, Inlay MA, Weissman IL, Murre C. E2A proteins maintain the hematopoietic stem cell pool and promote the maturation of myelolymphoid and myeloerythroid progenitors. *Proc Natl Acad Sci U S A*. 2009; 106:1930–1935. [PubMed: 19181846]
- Serbina NV, Pamer EG. Monocyte emigration from bone marrow during bacterial infection requires signals mediated by chemokine receptor CCR2. *Nat Immunol*. 2006; 7:311–317. [PubMed: 16462739]
- Shi C, Jia T, Mendez-Ferrer S, Hohl TM, Serbina NV, Lipuma L, Leiner I, Li MO, Frenette PS, Pamer EG. Bone marrow mesenchymal stem and progenitor cells induce monocyte emigration in response to circulating toll-like receptor ligands. *Immunity*. 2011; 34:590–601. [PubMed: 21458307]
- Shields AF, Grierson JR, Dohmen BM, Machulla HJ, Stayanoff JC, Lawhorn-Crews JM, Obradovich JE, Muzik O, Mangner TJ. Imaging proliferation in vivo with [F-18]FLT and positron emission tomography. *Nat Med*. 1998; 4:1334–1336. [PubMed: 9809561]
- Si Y, Tsou CL, Croft K, Charo IF. CCR2 mediates hematopoietic stem and progenitor cell trafficking to sites of inflammation in mice. *J Clin Invest*. 2010; 120:1192–1203. [PubMed: 20234092]
- Subramanian A, Tamayo P, Mootha VK, Mukherjee S, Ebert BL, Gillette MA, Paulovich A, Pomeroy SL, Golub TR, Lander ES, Mesirov JP. Gene set enrichment analysis: a knowledge-based approach for interpreting genome-wide expression profiles. *Proc Natl Acad Sci U S A*. 2005; 102:15545–15550. [PubMed: 16199517]
- Summers AR, Fischer MA, Stengel KR, Zhao Y, Kaiser JF, Wells CE, Hunt A, Bhaskara S, Luzwick JW, Sampath S, Chen X, Thompson MA, Cortez D, Hiebert SW. HDAC3 is essential for DNA replication in hematopoietic progenitor cells. *J Clin Invest*. 2013; 123:3112–3123. [PubMed: 23921131]
- Swirski FK, Nahrendorf M. Leukocyte behavior in atherosclerosis, myocardial infarction, and heart failure. *Science*. 2013; 339:161–166. [PubMed: 23307733]
- Swirski FK, Nahrendorf M, Etzrodt M, Wildgruber M, Cortez-Retamozo V, Panizzi P, Figueiredo JL, Kohler RH, Chudnovskiy A, Waterman P, Aikawa E, Mempel TR, Libby P, Weissleder R, Pittet MJ. Identification of splenic reservoir monocytes and their deployment to inflammatory sites. *Science*. 2009; 325:612–616. [PubMed: 19644120]
- Swirski FK, Pittet MJ, Kircher MF, Aikawa E, Jaffer FA, Libby P, Weissleder R. Monocyte accumulation in mouse atherogenesis is progressive and proportional to extent of disease. *Proc Natl Acad Sci U S A*. 2006; 103:10340–10345. [PubMed: 16801531]
- Tacke F, Alvarez D, Kaplan TJ, Jakubzick C, Spanbroek R, Llodra J, Garin A, Liu J, Mack M, van Rooijen N, Lira SA, Habenicht AJ, Randolph GJ. Monocyte subsets differentially employ CCR2, CCR5, and CX3CR1 to accumulate within atherosclerotic plaques. *J Clin Invest*. 2007; 117:185–194. [PubMed: 17200718]
- Takizawa H, Regoes RR, Boddupalli CS, Bonhoeffer S, Manz MG. Dynamic variation in cycling of hematopoietic stem cells in steady state and inflammation. *J Exp Med*. 2011; 208:273–284. [PubMed: 21300914]
- Tusher VG, Tibshirani R, Chu G. Significance analysis of microarrays applied to the ionizing radiation response. *Proc Natl Acad Sci U S A*. 2001; 98:5116–5121. [PubMed: 11309499]
- Wilson A, Laurenti E, Oser G, van der Wath RC, Blanco-Bose W, Jaworski M, Offner S, Dunant CF, Eshkind L, Bockamp E, Lio P, Macdonald HR, Trumpp A. Hematopoietic stem cells reversibly switch from dormancy to self-renewal during homeostasis and repair. *Cell*. 2008; 135:1118–1129. [PubMed: 19062086]

- Yamamoto R, Morita Y, Ooehara J, Hamanaka S, Onodera M, Rudolph KL, Ema H, Nakauchi H. Clonal analysis unveils self-renewing lineage-restricted progenitors generated directly from hematopoietic stem cells. *Cell*. 2013; 154:1112–1126. [PubMed: 23993099]
- Yang L, Bryder D, Adolfsson J, Nygren J, Månsson R, Sigvardsson M, Jacobsen SE. Identification of Lin(–)Sca1(+)kit(+)CD34(+)Flt3– short-term hematopoietic stem cells capable of rapidly reconstituting and rescuing myeloablated transplant recipients. *Blood*. 2005; 105:2717–23. 2005. [PubMed: 15572596]
- Young JC, Wu S, Hansteen G, Du C, Sambucetti L, Remiszewski S, O’Farrell AM, Hill B, Lavau C, Murray LJ. Inhibitors of histone deacetylases promote hematopoietic stem cell self-renewal. *Cytotherapy*. 2004; 6:328–336. [PubMed: 16146885]
- Yvan-Charvet L, Pagler T, Gautier EL, Avagyan S, Siry RL, Han S, Welch CL, Wang N, Randolph GJ, Snoeck HW, Tall AR. ATP-binding cassette transporters and HDL suppress hematopoietic stem cell proliferation. *Science*. 2010; 328:1689–1693. [PubMed: 20488992]
- Zaheer A, Lenkinski RE, Mahmood A, Jones AG, Cantley LC, Frangioni JV. In vivo near-infrared fluorescence imaging of osteoblastic activity. *Nat Biotechnol*. 2001; 19:1148–1154. [PubMed: 11731784]
- Zhang J, Leiderman K, Pfeiffer JR, Wilson BS, Oliver JM, Steinberg SL. Characterizing the topography of membrane receptors and signaling molecules from spatial patterns obtained using nanometer-scale electron-dense probes and electron microscopy. *Micron*. 2006; 37:14–34. [PubMed: 16081296]

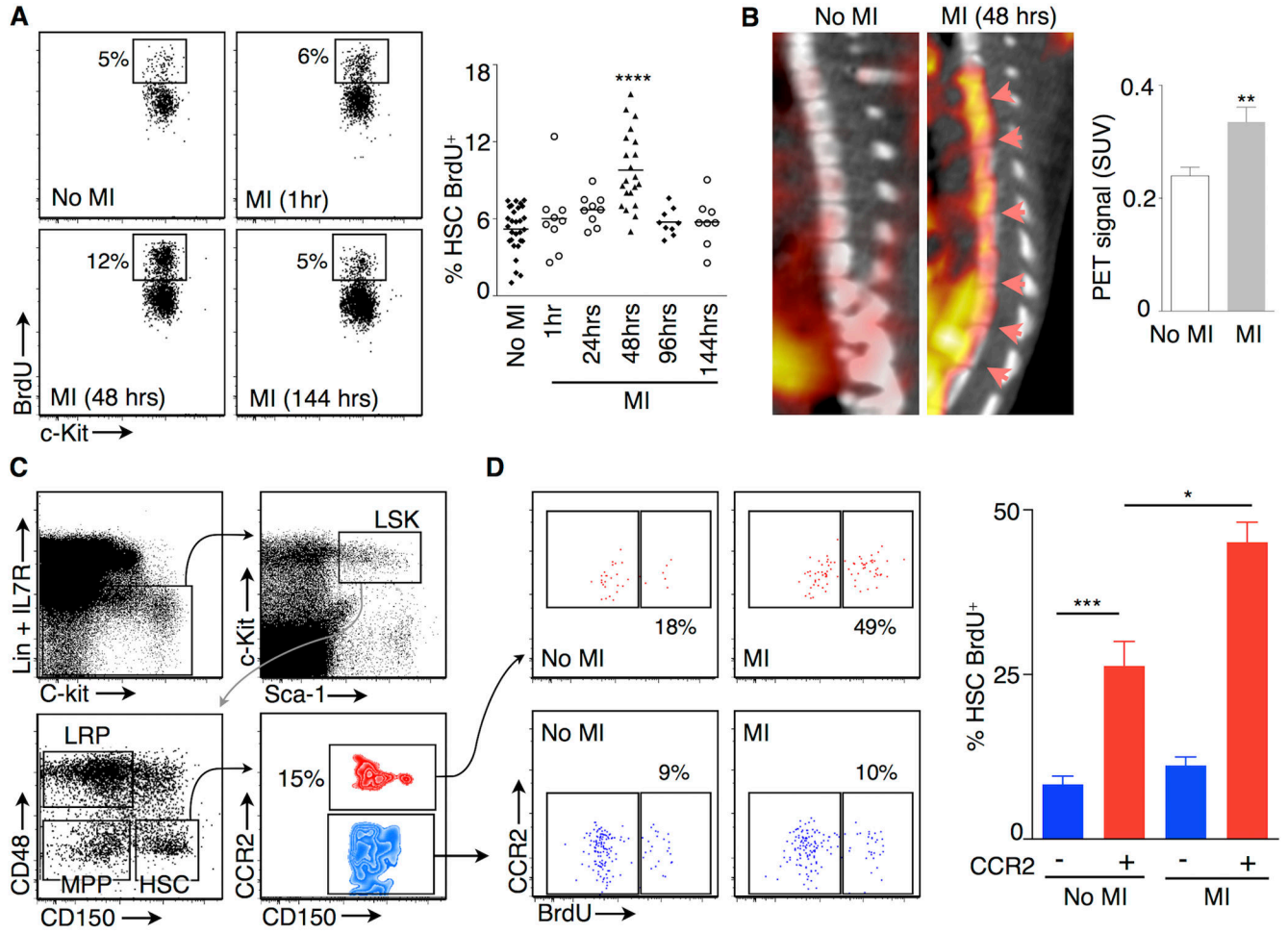


**Figure 1. Activation of HSPC after MI**

(A) CD48<sup>-</sup>CD150<sup>+</sup> HSC proliferation measured by BrdU incorporation with flow cytometry in steady state (No MI) and at different time points after MI (permanent coronary ligation, n=8–29 per group). Hours refer to the time of BrdU injection after coronary ligation.

(B) Proliferation imaged by <sup>18</sup>F-FLT PET/CT in bone marrow 2 days after MI. Arrow heads indicate increased PET signal in the vertebral marrow (n=5–6 per group).

(C) Flow cytometric gating strategy for CCR2<sup>+</sup> CD150<sup>+</sup> CD48<sup>-</sup> LSK, LRP and MPP.

(D) Proliferation of CD48<sup>-</sup> CD150<sup>+</sup> CCR2<sup>+</sup> and CCR2<sup>-</sup> LSK in steady state and 48 hours after MI (n=5–17 per group) in mice. Data are shown as mean ± SEM, \* *P* < 0.05, \*\* *P* < 0.01, \*\*\* *P* < 0.001, \*\*\*\* *P* < 0.0001. See also Figure S1.

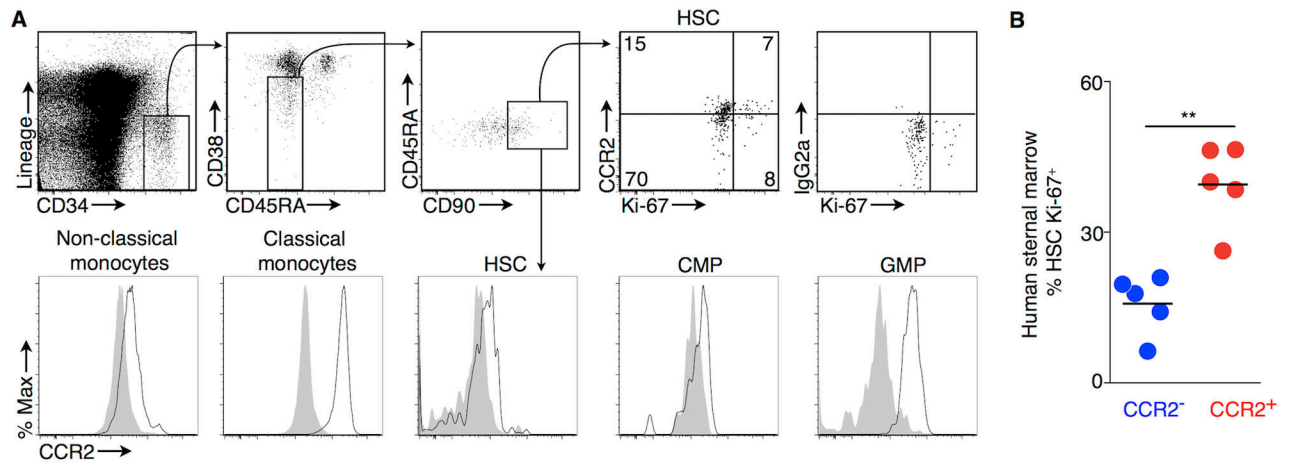


**Figure 2. Human CCR2<sup>+</sup> expression in HSC**

(A) CCR2 expression on human non-classical monocytes and classical monocytes in the blood, and CMP, GMP and HSC in the bone marrow harvested from the sternum during open heart surgery. The gating strategy for human HSC is shown. The upper most right panel shows isotype control staining for the CCR2 antibody.

(B) Proliferation of human CCR2<sup>+</sup> and CCR2<sup>-</sup> HSPC (n=5 per group). Data are shown as mean ± SEM, \*\*  $P < 0.01$ . Patient characteristics are listed in Table S1.



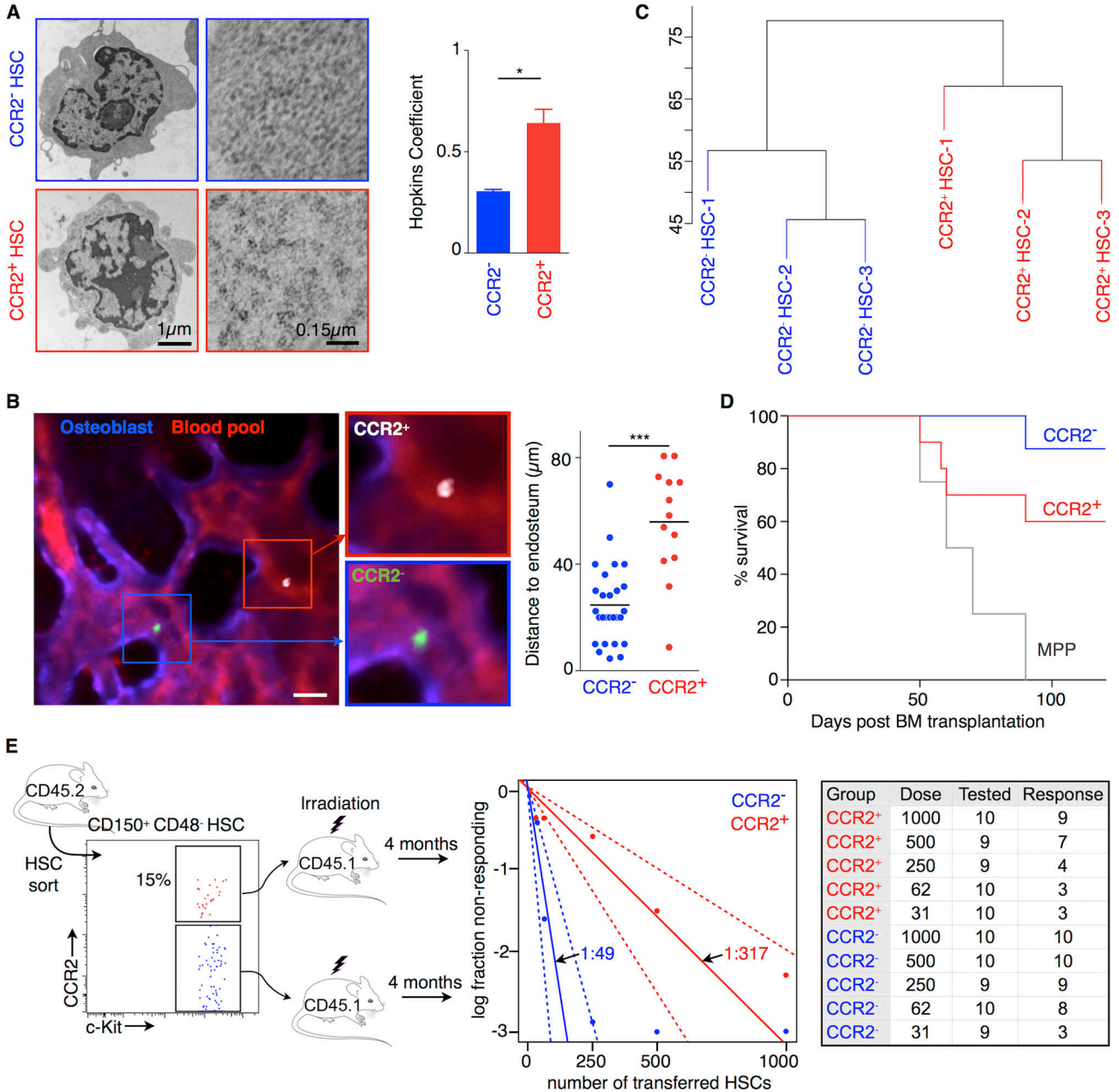


**Figure 3. CCR2<sup>+</sup> HSPC phenotype, location and function**

(A) Electron microscopy images of cell subsets (left panel) and magnified cytosol showing distribution of ribosomes (right panel). The bar graph shows ribosome aggregation in subsets (one tail Wilcoxon rank sum test,  $p=0.036$ ) ( $n=6$  ROIs in 3 CCR2<sup>+</sup> and  $n=13$  ROIs in 5 CCR2<sup>-</sup> HSPC).

(B) DiO-labelled CCR2<sup>-</sup> and DiD-labelled CCR2<sup>+</sup> CD150<sup>+</sup> CD48<sup>-</sup> LSK were imaged in the skull with intravital microscopy 1 day after transfer ( $n=13-27$  cells in 2 mice per group). DiO-labelled CCR2<sup>-</sup> HSC are green, DiD-labelled CCR2<sup>+</sup> HSPC are white, blood pool is red and osteoblasts are blue.

(C) Hierarchical clustering dendrogram based on whole-transcriptome microarray data of CCR2<sup>+</sup> and CCR2<sup>-</sup> CD150<sup>+</sup> CD48<sup>-</sup> LSK sorted from steady state bone marrow (3 replicates per group).

(D) Survival curve of lethally irradiated mice reconstituted with either CCR2<sup>-</sup> (n=8), CCR2<sup>+</sup> (n=10) CD150<sup>+</sup> CD48<sup>-</sup> LSK or MPP (n=4).

(E) Limiting dilution assay determined functional HSC frequency among CCR2<sup>-</sup> and CCR2<sup>+</sup> CD150<sup>+</sup> CD48<sup>-</sup> LSK in wild type bone marrow. Multi-lineage blood chimerism of 0.1% or higher served as cut off value to determine responders ( $p < 0.001$  for difference in frequency). Table lists dilution steps, numbers of mice analyzed 4 months after HSC transfer, and number of responders.

Data are shown as mean  $\pm$  SEM, \*  $P < 0.05$ , \*\*\*  $P < 0.001$ . See also Figure S2 and Table S2.

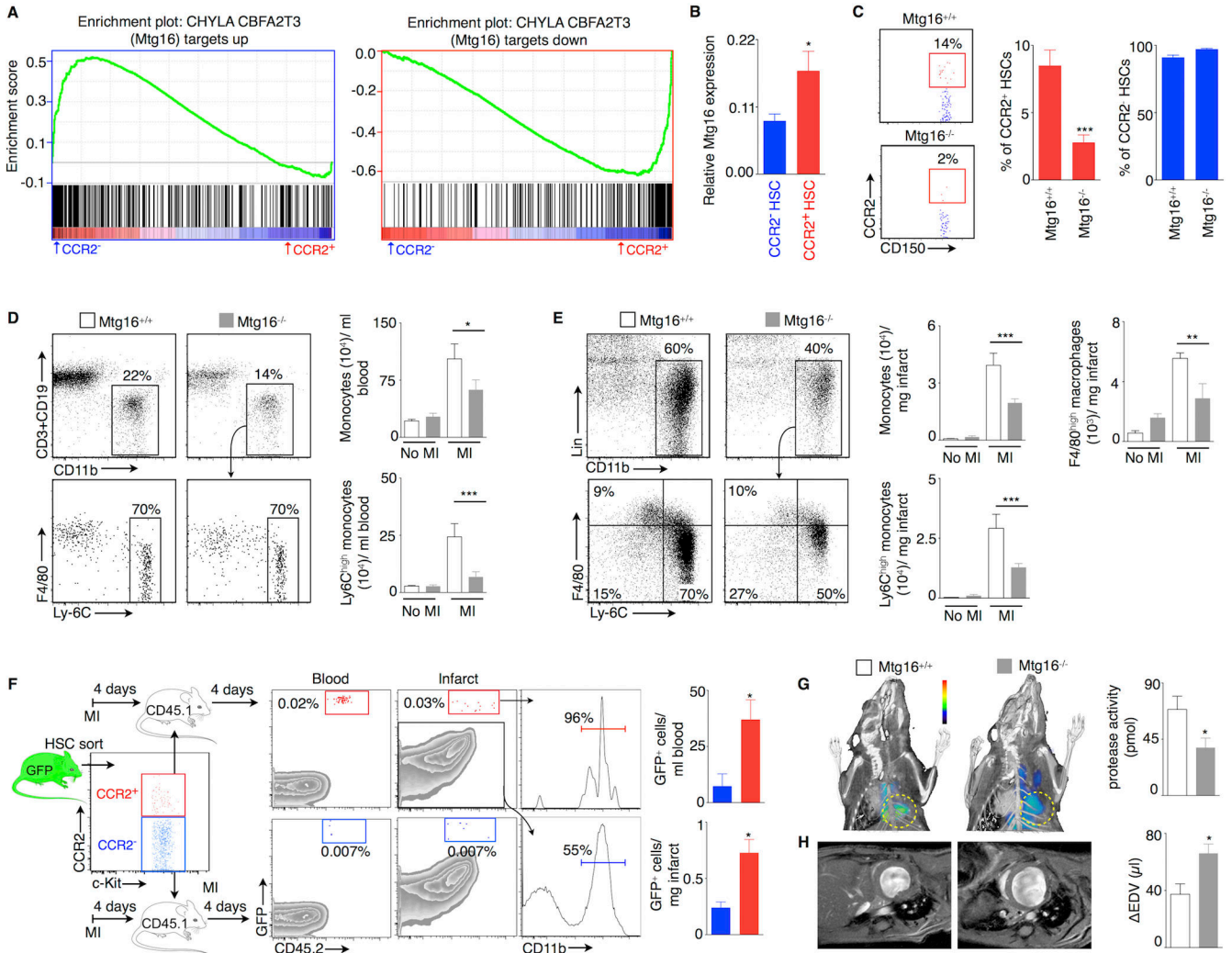


**Figure 4. Role of Mtg16 in myelopoiesis**

(A) Gene-set enrichment analysis showing that CCR2<sup>+</sup> HSPC express genes that are downregulated in hematopoietic stem and progenitor cells in *Mtg16*<sup>-/-</sup> mice, while CCR2<sup>-</sup> HSC express genes are upregulated in *Mtg16*<sup>-/-</sup> (false discovery rate q-value <0.0001 in both cases).  
 (B) Mtg16 mRNA expression in HSC normalized to Gapdh (n=6 per group).  
 (C) Percentage of CCR2<sup>+</sup> and CCR2<sup>-</sup> CD150<sup>+</sup> CD48<sup>-</sup> LSK in wild type and *Mtg16*<sup>-/-</sup> mice in steady state (n=7–8 per group).  
 (D and E) FACS quantification of myeloid cells 3 days after MI in the blood (D) and infarct (E) of wild type and *Mtg16*<sup>-/-</sup> mice (n=4–6 per group).  
 (F) Seven thousand CCR2<sup>+</sup> or CCR2<sup>-</sup> CD150<sup>+</sup> CD48<sup>-</sup> LSK were sorted from GFP<sup>+</sup> bone marrow and adoptively transferred into CD45.1 C57B/6 on day 4 after MI. Four days after transfer, progeny of GFP<sup>+</sup> cells were analyzed in the blood and infarct (n=4 per group).  
 (G) In vivo protease imaging in wild type and *Mtg16*<sup>-/-</sup> mice on day 7 after MI (infarct indicated by yellow circle) (n=10–12 per group).

(H) Change in end-diastolic volume (EDV) between day 1 and 21 after MI in wild type and *Mtg16<sup>-/-</sup>* mice measured with cardiac MRI. Original MR images show representative enddiastolic mid-ventricular short axis view 21 days after MI (n=6–7 per group). Data are shown as mean  $\pm$  SEM, \*  $P < 0.05$ , \*\*  $P < 0.01$ , \*\*\*  $P < 0.001$ . See also Figure S3.

Author Manuscript

Author Manuscript

Author Manuscript

Author Manuscript

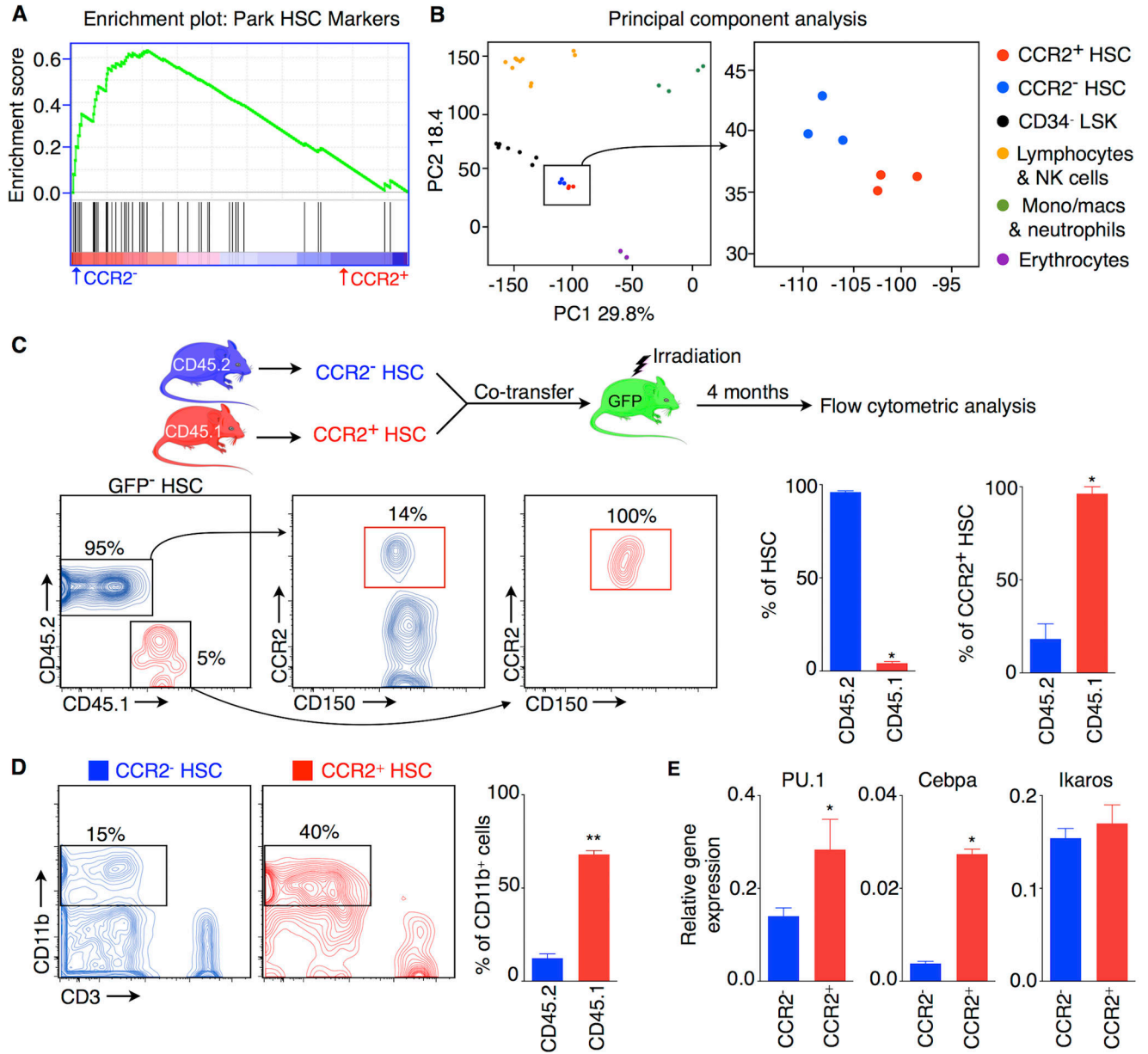


**Figure 5. Lineage relationship between CCR2<sup>+</sup> and CCR2<sup>-</sup> CD150<sup>+</sup> CD48<sup>-</sup> LSK**

(A) Gene-set enrichment analysis for HSC genes shows enrichment in CCR2<sup>-</sup> HSC (FDR qvalue= 0.001).

(B) Principal components analysis. Projection of CCR2<sup>+</sup> and CCR2<sup>-</sup> CD48<sup>-</sup> CD150<sup>+</sup> LSK into the same space as mouse HSC, leukocytes and erythrocytes shows differentiation of CCR2<sup>+</sup> CD150<sup>+</sup> CD48<sup>-</sup> LSK along the myeloid lineage.

(C) Upper panel: Experimental design for competitive bone marrow reconstitution with 100 CCR2<sup>+</sup> and CCR2<sup>-</sup> CD150<sup>+</sup> CD48<sup>-</sup> LSK. Lower panel: plots showing HSC chimerism in the bone marrow and percentage of CCR2<sup>+</sup> CD150<sup>+</sup> CD48<sup>-</sup> LSK derived from transferred cells. The bar graphs depict quantified flow cytometric data (n=4 per group).

(D) Blood chimerism in myeloid cells derived from transferred HSC 4.5 months after bone marrow reconstitution (n=3 per group).

(E) mRNA levels of myeloid (PU.1 and Cebpa) and lymphoid (Ikaros) transcription factors in FACS-isolated CCR2<sup>+</sup> and CCR2<sup>-</sup> CD150<sup>+</sup> CD48<sup>-</sup> LSK, normalized to Gapdh (n=3–10 per group).

Data are shown as mean  $\pm$  SEM, \*  $P < 0.05$ , \*\*  $P < 0.01$ . See also Figure S4.

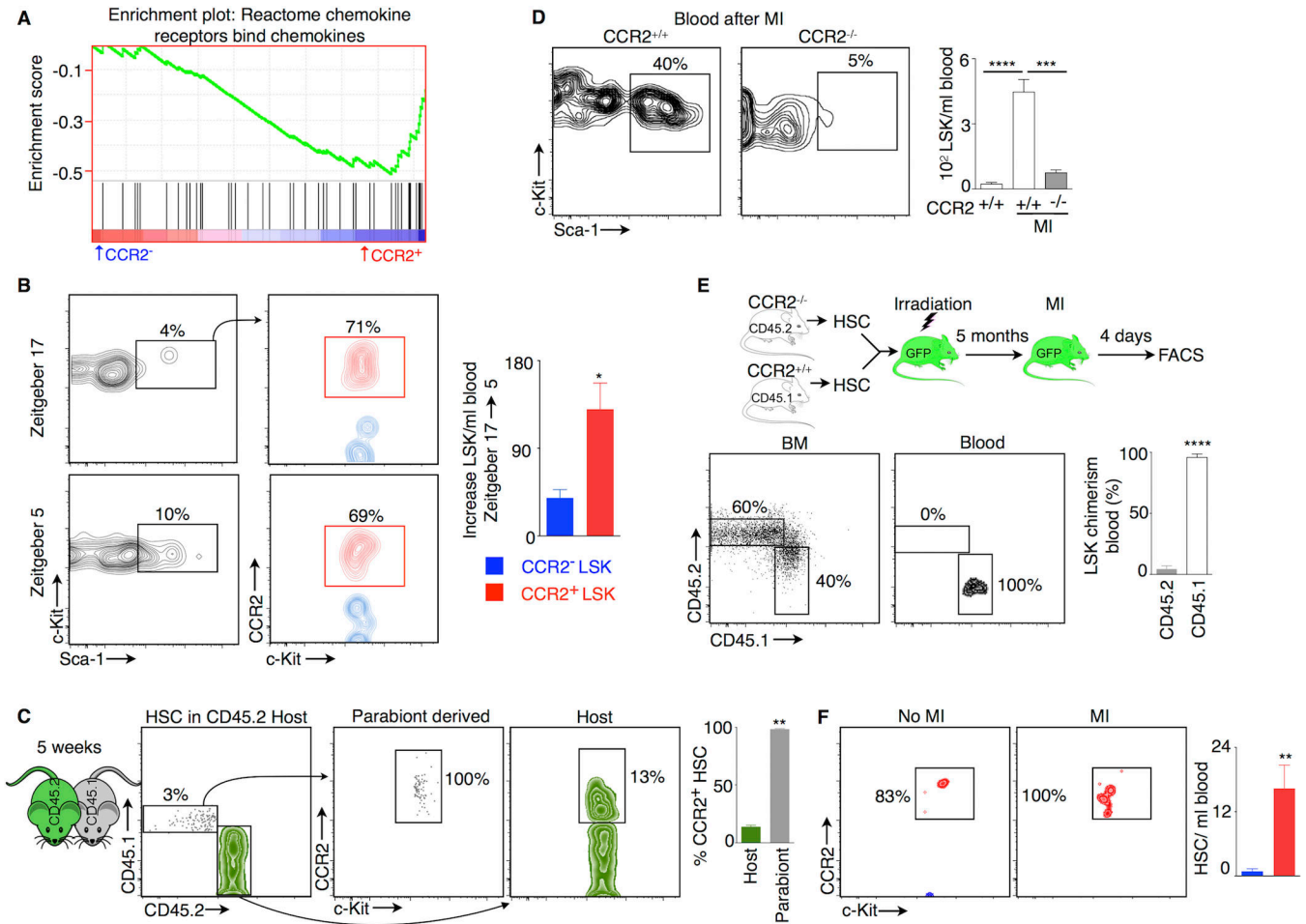


**Figure 6. Migration of CCR2<sup>+</sup> CD150<sup>+</sup> CD48<sup>-</sup> LSK from the bone marrow in steady state and after MI**

(A) Gene-set enrichment analysis for chemokines and chemokine receptors shows enrichment in CCR2<sup>+</sup> CD150<sup>+</sup> CD48<sup>-</sup> LSK (FDR q-value=0.01).

(B) Percentage of CCR2<sup>+</sup> and CCR2<sup>-</sup> CD150<sup>+</sup> CD48<sup>-</sup> LSK in the blood during steady state at Zeitgeber 17 (midnight) and Zeitgeber 5 (noon) (n=4 per group).

(C) CD45.1 and CD45.2 mice were analyzed after 5 weeks of parabiosis. Only CCR2<sup>+</sup> CD150<sup>+</sup> CD48<sup>-</sup> LSK migrated to the other bone marrow of the other parabiont. The plots and the bar graph depict % of CCR2<sup>+</sup> host and migratory CD150<sup>+</sup> CD48<sup>-</sup> LSK in the bone marrow (n=5 per group).

(D) LSK in blood in CCR2<sup>-/-</sup> and wild type mice 4 days after inducing myocardial infarction (MI) (n=5–12 per group).

(E) Upper panel: Experimental design to investigate CCR2-dependent emigration from the bone marrow after MI. Lower panel: % of LSK chimerism in the blood (normalized to bone marrow chimera) 4 days after MI (n=5 per group).

(F) Post-MI HSC release into blood is dominated by CCR2<sup>+</sup> CD150<sup>+</sup> CD48<sup>-</sup> LSK. FACS plots are gated on HSC. The bar graph depicts the increase of absolute HSC numbers in blood from steady state to day 3 after MI (n=8–9 per group).

Data are shown as mean  $\pm$  SEM, \*  $P < 0.05$ , \*\*  $P < 0.01$ , \*\*\*  $P < 0.001$ , \*\*\*\*  $P < 0.0001$ .  
See also Figure S5.

Author Manuscript

Author Manuscript

Author Manuscript

Author Manuscript



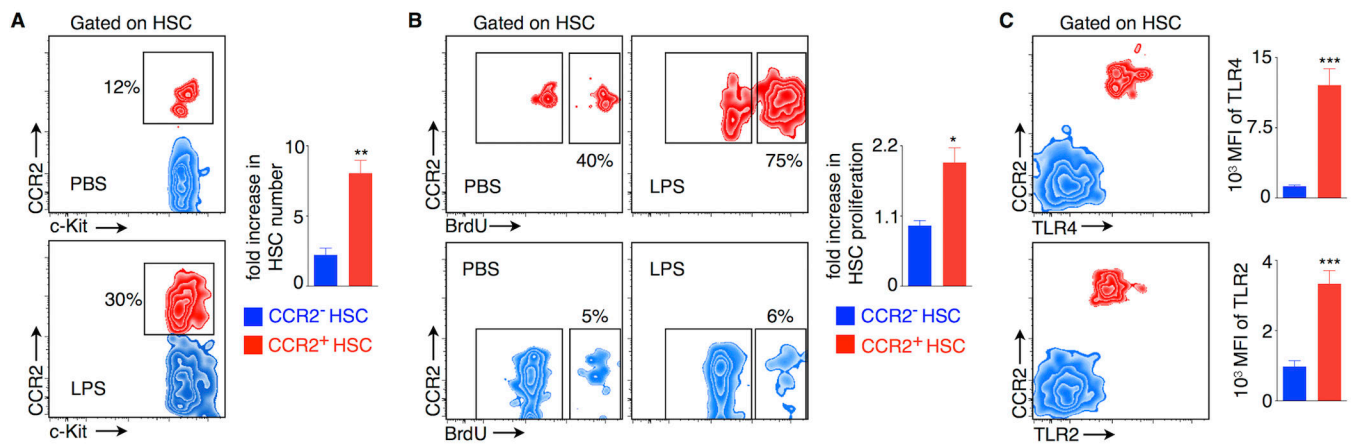


### Figure 7. CCR2<sup>+</sup> HSPC after LPS treatment

(A) Fold change of CCR2<sup>+</sup> and CCR2<sup>-</sup> CD150<sup>+</sup> CD48<sup>-</sup> LSK number in bone marrow of LPS injected mice compared to PBS-injected controls at 4 hours after injection (n=4 per group).

(B) Fold change of proliferation 4 hours after injecting LPS (n=6 per group).

(C) Steady state TLR4 and TLR2 expression levels on HSC (n=9 per group). Data are shown as mean  $\pm$  SEM, \*  $P < 0.05$ , \*\*  $P < 0.01$ , \*\*\*  $P < 0.001$ . See also Figure S6.